

## Corrosion of iron: A study for radioactive waste canisters

S. Ben Lagha <sup>a,b,\*</sup>, D. Crusset <sup>b</sup>, I. Mabille <sup>a</sup>, M. Tran <sup>a</sup>, M.C. Bernard <sup>c</sup>, E. Sutter <sup>a</sup>

<sup>a</sup> *Laboratoire de Génie des Procédés Plasmas et Traitements de Surface (EA349/UPMCI/ENSCP), 11 rue Pierre et Marie Curie, 75231 Paris cedex 05, France*

<sup>b</sup> *ANDRA, 117 rue Jean Monnet 92298 Châtenay, Malabry cedex, France*

<sup>c</sup> *Laboratoire des Interfaces et Systèmes Electrochimiques – (UPR15/UPMCI/CNRS), 4 place Jussieu, 75252 Paris cedex 05, France*

### Abstract

The purpose of this study is to examine the risks of atmospheric corrosion of steel waste canisters following their deep geological disposal in the temperature range from 303 to 363 K. The work was performed using iron samples deposited as thin films on a quartz crystal microbalance (QCM) and disposed in a climatic chamber. The experiments showed that, in the temperature under study (298–363 K), the mass increase due to the formation of oxide/hydroxide rose sharply above 70%  $R_H$ , as is commonly observed at room temperatures, indicating that the phenomenon remains electrochemical in nature. Ex situ Raman spectrometric analyses indicate the formation of magnetite, maghemite and oxyhydroxides species in the 298–363 K temperature range, and for oxygen contents above 1 vol.%, whereas only  $Fe_3O_4$  and  $\gamma-Fe_2O_3$  are detected at 363 K. In this work, the kinetics of the rust growth is discussed, on the bases of the rate of mass increase and of the composition of the rust, as a function of the climatic parameters and the oxygen content of the atmosphere.

© 2007 Elsevier B.V. All rights reserved.

PACS: 82.45.Bb; 68.47.De

### 1. Introduction

In the context of deep geologic disposal of radioactive waste canisters, the estimation of the corrosion rate of these metallic canisters has to be made over a period of thousand years and more [1]. The wastes could be packaged in containers made of carbon steel and first disposed in long-term initially dry disposal in metallic liners. The temperature of the

canister is estimated to reach 363 K during the first fifty years, then to progressively decrease to reach 303 K after about 1000 years. The atmospheric environment of the canister is likely to become more and more humid due to eventual lack of tightness of the liner. The oxygen content of the disposal gallery is initially equal to the atmospheric content (20% in volume), but anoxic conditions will be rapidly established, since oxygen will be scavenged by reaction with the steel of the container, or with any mineral or organic material present in the environment. Thus the exact atmospheric conditions (temperature, relative humidity, composition) at a given time remain largely unknown. As a matter of fact, some deterioration of the containers could occur

\* Corresponding author. Address: Laboratoire de Génie des Procédés Plasmas et Traitements de Surface, (EA349/UPMCI/ENSCP), 11 rue Pierre et Marie Curie, 75231 Paris cedex 05, France. Tel.: +33 144276720; fax: +33 143263738.

E-mail address: [sabah-benlagha@enscp.fr](mailto:sabah-benlagha@enscp.fr) (S.B. Lagha).

in conditions of temperature, relative humidity and oxygen concentration which may vary with time. The mechanism of the corrosion processes in these conditions has thus to be improved in a temperature range (298–363 K), different values of relative humidity between 0% and 90% and oxygen concentrations from anoxic to 20% in volume.

Wet corrosion of materials under a thin water film is usually considered to be of electrochemical nature. Nevertheless electrochemical measurements in very thin electrolyte layers (<1000  $\mu\text{m}$ ) are very difficult to realize, particularly at 363 K. Thus in the literature, the corrosion behaviour of steel at high temperature has often been investigated using analytical methods such as Raman spectroscopy, infrared spectroscopy, X-ray diffraction, X-ray photoelectron spectroscopy [2–5], or using weight–mass measurements [6]. In these references, high temperature studies have generally been performed in bulk solutions and at high pressure and do not reproduce the behaviour of steel under a thin layer electrolyte. The use of a quartz crystal microbalance (QCM) appears thus to be a more adapted method for reproducing experimental conditions close to the conditions of the disposal, since it allows following the mass gain of a metallic surface in contact with a very thin water layer at atmospheric pressure. In

the present work, a QCM was used for which the classical gold surface has been covered by an iron film (0.33  $\mu\text{m}$  thickness) deposited through physical vapour deposition, disposed in a climatic chamber in order to follow the mass gain of the metallic samples placed in it, as a function of the relative humidity, the temperature between 298 and 363 K, and the concentration of oxygen.

## 2. Experimental

The atmospheric corrosion tests were performed in a climatic chamber during maximum exposure times of 14–20 days. The samples were exposed in the chamber in which the temperature and the relative humidity ( $R_H$ ) was maintained constant and continuously monitored during each experiment. Relative humidity was obtained by mixing a water saturated nitrogen/oxygen flow with a dry nitrogen flow in the proper proportions, i.e. carbon dioxide was excluded from the ‘synthetic’ air. The amount of oxygen varied from the atmospheric concentration (20% in volume) to concentrations of about 1 vol.%. The mixed air stream entered the climatic chamber with a flow of 40 L per hour. The experimental device is represented in Fig. 1. The quartz samples (1.37  $\text{cm}^2$  exposed area) purchased from

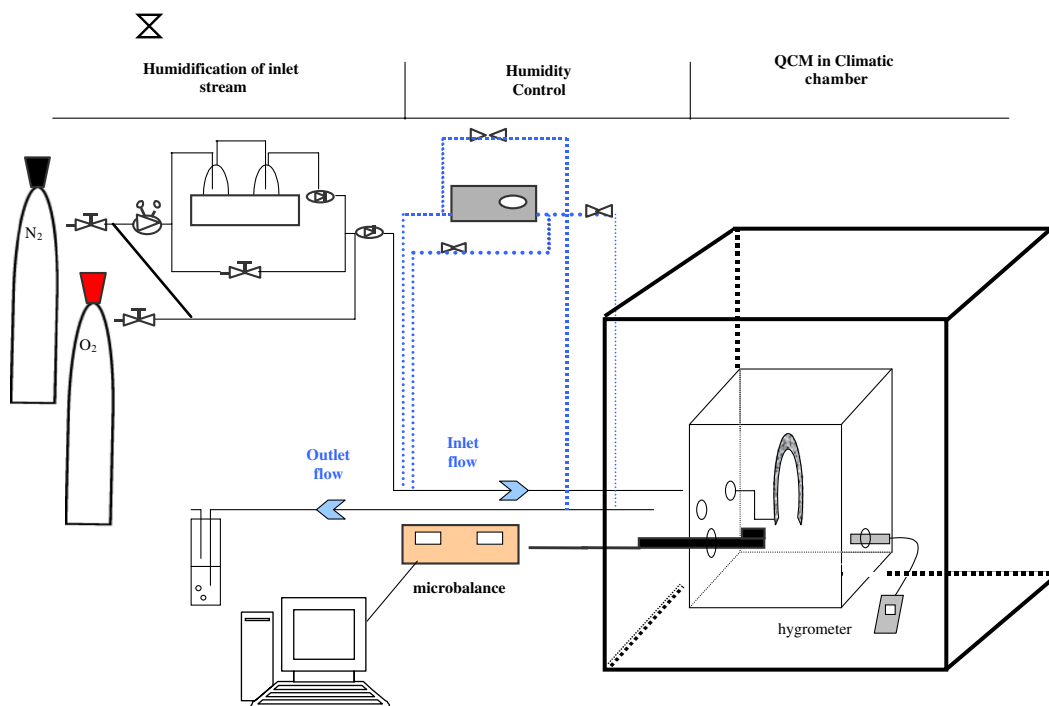


Fig. 1. Experimental device for the study of atmospheric corrosion at different temperatures, relative humidity and oxygen concentrations.

MAXTEK Inc., were 5 MHz AT-cut Au/Ti quartz crystals with a polished iron deposit of about  $0.33 \mu\text{m}$  (PVD deposition performed by MAXTEK Inc.). During QCM measurements, the frequency of the quartz can be measured with an accuracy of 0.1 Hz. It changes in direct proportion to changes in mass, leading to a mass change sensitivity of about  $10^{-8} \text{g cm}^{-2}$ . Before exposure, the samples were rinsed with ethanol (60%) and deionised water, then dried with air. Preliminary electrochemical tests showed that the corrosion rate of the iron deposit in 0.25 M  $\text{K}_2\text{SO}_4$  was the same as for a bulk steel electrode ( $i_{\text{cor}} \sim 2 \times 10^{-5} \text{A cm}^{-2}$ ).

After each experiment, the quartz samples were analysed by Raman spectrometry using a LAB-RAM spectrometer from JOBIN-YVON HORIBA. The red line at 632.8 nm of a He–Ne laser was used. A confocal OLYMPUS BX40 microscope with a hole fixed at  $200 \mu\text{m}$  lead to a lateral resolution of respectively 5 and  $2 \mu\text{m}$ .

### 3. Results and discussion

#### 3.1. Corrosion under atmospheric conditions

##### 3.1.1. Influence of relative humidity at 343 K

The influence of the relative humidity is reported for a gas composition of 20%  $\text{O}_2$ –80%  $\text{N}_2$ , at 343 K which is close to the highest temperature reached by the canisters (363 K). The mass change with time of the QCM during exposure is plotted in Fig. 2(a) for  $R_{\text{H}}$  values varying from 50% to 90%. In the present work, all the experimental results are reported in terms of areal mass density ( $\text{g cm}^{-2}$ ) taking into account the geometric area of  $1.37 \text{cm}^2$  and neglecting the surface roughness factor. Three kinetic

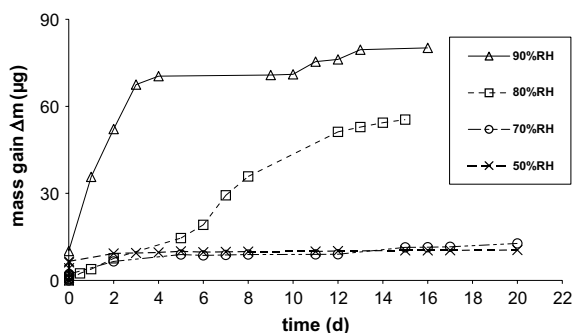


Fig. 2(a). Mass gain of the quartz with an iron deposit as a function of time. Influence of the  $R_{\text{H}}$  value at 343 K and 20% of oxygen content. Experimental results and fitted curves.

periods appear during the growth of the corrosion products.

The first period (about 1 h) is very short compared to the total exposure time and the QCM shows a small increase in the mass. This period is attributed to the adsorption of water molecules on the metallic surface. According to Aastrup et al. [7], water is adsorbed in form of clusters and adsorption is not homogeneous on the whole surface. A complete monolayer of water has been reported to change the mass by about  $30 \text{ng cm}^{-2}$  [8]. In the present work, the increase in mass during the first period at 90%  $R_{\text{H}}$  was between 0.7 and  $1.0 \mu\text{g cm}^{-2}$  (not shown here). If the mass of the oxide spontaneously formed at the iron surface is neglected, and if the geometric area of the quartz is considered, approximately 23–33 monolayers of water molecules should be deposited on the iron surface in these conditions. According to [8], an initial adsorption of 10–20 monolayers of water, is the minimum amount of water necessary for electrochemical reactions to take place, so that corrosion may proceed via such reactions in the present work.

As the mass variation of the QCM was followed during two weeks, it was not focused on the initial mass increase which was considered as negligible in comparison with the mass gain due to oxide/hydroxide formation.

The second period corresponds to the growth of the corrosion layer at the surface of the metal and spreads over 3–10 days. During this period, the rate of mass increase ( $r_2$ ) is the highest among the three periods. Fig. 2(a) clearly shows that at 343 K the mass due to oxide/hydroxide formation increases with relative humidity and increases dramatically for  $R_{\text{H}}$  values above 70%. From the measurements reported in Fig. 2(a), the rate of increase of the oxide thickness  $r_2$  could be calculated according to

$$r_2 = \frac{\Delta m}{\Delta t \times \rho \times s}, \quad (1)$$

with  $\Delta m$  the mass gain,  $\Delta t$  the duration of the second period,  $s$  the geometric surface ( $1.37 \text{cm}^2$ ), and  $\rho$  the mean value of  $5 \text{g cm}^{-3}$  for the density of the oxide.

An exponential rate of growth as a function of  $R_{\text{H}}$  can be determined according to  $r_2 = 1.2 \times 10^{-2} \exp(0.086 R_{\text{H}})$  at 343 K, with  $r_2$  in  $\mu\text{m yr}^{-1}$  and for  $R_{\text{H}}$  values between 50% and 90% (see Fig. 2(b)).

The oxide thickness obtained in this work after 4 days at 90%  $R_{\text{H}}$  has been compared to the oxide

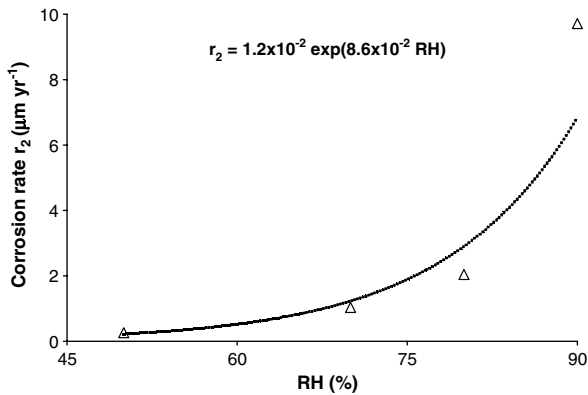


Fig. 2(b). Corrosion layer growth rate during period 2 as a function of the value of relative humidity.

thickness reported by Mabuchi et al. [6] after 4 days experiments in bulk water at 333 K in the presence of 2.5 ppm of dissolved oxygen. The thickness of 1.5  $\mu\text{m}$  estimated by these authors is about 4 times higher than in this work (in Fig. 2(a), a mass of 70  $\mu\text{g}$  corresponds to a thickness of 0.4  $\mu\text{m}$ ). This different behaviour between oxide layer formed in bulk solution and oxide layer formed under a thin water layer shows that electrochemical reactions are more difficult to occur in the presence of adsorbed layers of water.

During the third period ranging from 5 days to 15 days, the rate of mass gain is slowed down. In Fig. 3, representing the photographs of a quartz before and after 15 days of exposure at 343 K and 80%  $R_H$ , we clearly observe that the corrosion is not uniform at the surface of the iron deposit, corroborating that water adsorption on the metallic surface is initially not uniform but probably in form of clusters. A rough optical estimation of the surface coverage by the oxide is reported in Table 1. The surface coverage is about 9% at 70%  $R_H$  and reaches

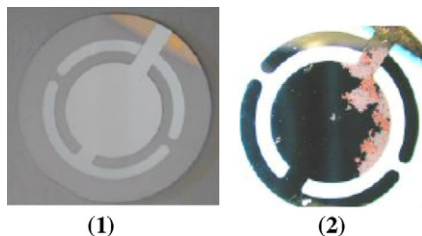


Fig. 3. Photographs of a quartz with an iron deposit: (1) before exposition (2) after exposition at 343 K in the presence of 20%  $\text{O}_2$  and 80%  $R_H$  during 15 days. Note the non-uniform corrosion after exposure in the climatic chamber.

Table 1

Final mass gain and surface coverage after two weeks of exposure as a function of relative humidity and for 343 K–20%  $\text{O}_2$

Relative humidity (%)	Mass gain ( $\mu\text{g}$ )	Surface coverage (%)
90	71	20
80	46	20
70	4	9
50	2	Traces

20% at 80%  $R_H$ , indicating that the corrosion layer spreads out at the surface in this  $R_H$  range. On the other hand, when the  $R_H$  value further increases from 80% to 90%, the surface coverage keeps a near constant value, though the mass further increases, as a result of a growth in thickness of the film.

At 50% and 70%  $R_H$ , a mass stabilization is clearly observed after 5 days of immersion in Fig. 2(a). Assuming an uniform coverage of the surface, the estimated thickness of the oxide layer would be between 10 and 20 nm after 5 days of exposure. This value is of the same order of magnitude as the values reported at 373 K after 24 h of exposure, by Sato et al. [2] who obtained a constant thickness of 4.5 nm in dry air and a maximum thickness of 18 nm in air containing water vapour at a pressure of  $2 \times 10^{-4}$  Pa. A third rate of mass increase ( $r_3$ ) can then be estimated from the slope of the curve in the third period and the corresponding rate of iron consumption  $r_{3\text{Fe}}$  is

$$r_{3\text{Fe}} \sim 0.04 \mu\text{m yr}^{-1} \text{ for } 50\% R_H \text{ and}$$

$$r_{3\text{Fe}} \sim 0.23 \mu\text{m yr}^{-1} \text{ for } 70\% R_H.$$

At higher  $R_H\%$  values, the behaviour of the deposit in the third period is less evident. The third period ( $\Delta t > 5$  d) of the curve obtained for  $R_H$  value of 90% is not significant. In this region the iron film was totally consumed after five days at the places where corrosion took place. Nevertheless, exposure times above five days provide interesting insights into the mechanism of growth of the corrosion layer, as it appears that the surface zones initially not corroded stay further undamaged over a longer period. A protective film is likely to be present at the uncorroded area, and to hinder any reaction between the iron surface and the water film. According to former studies [2,6], this protective film should be a thin compact magnetite layer. It has been reported [9] that surface properties such as roughness have a substantial influence on water adsorption characteristics. Therefore the values of

the surface coverage here observed at the mirror-like iron deposit may be different in the case of bulk steel samples.

At 80%  $R_H$ , the curve (Fig. 2(a)) showing the mass gain as a function of time is significant, since the consumed amount of iron is lower than at 90%  $R_H$ , and since the gold substrate of the QCM was never observed in this condition. As was observed at lower  $R_H$  values, a slowing down of the rate of mass increase is observed but it occurs only after 10 days of exposure and it is not as well pronounced as in the case of 50% and 70%  $R_H$ .

The analysis of the corrosion layers formed at the different  $R_H$  values was performed using Raman Spectrometry (Fig. 4) in order to interpret the kinetic results. Table 2 shows that magnetite  $Fe_3O_4$  and maghemite  $\gamma-Fe_2O_3$  are present at all of the tested  $R_H$  values, whereas hydroxides (goethite  $\alpha-FeOOH$  and lepidocrocite  $\gamma-FeOOH$ ) were only detected for  $R_H$  values equal or above 70%. Magnetite and maghemite were localized near the metallic surface, whereas hydroxides were mainly present in the upper part of the rust layer. These observations are very close to those made by Maslar et al. [5] who also identified in water at 374 K and at a pressure of 25.1 MPa, the presence of  $Fe_3O_4$ ,  $\gamma-Fe_2O_3$ ,  $\gamma-FeOOH$ , but also of  $\alpha-Fe_2O_3$ . This later oxide (hematite) was never observed in the present work, whatever the experimental conditions.

From the results given above, the rate of corrosion at 50%  $R_H$  can be neglected. The critical value of 60% for the relative humidity has often been

Table 2

Oxides and hydroxides phases detected by Raman spectroscopy for experiments performed at 343 K

Relative humidity (%)	Phases detected by Raman spectroscopy
50	$Fe_3O_4$ $\gamma-Fe_2O_3$
70	$Fe_3O_4$ $\gamma-FeOOH$ $\gamma-Fe_2O_3$
80	$Fe_3O_4$ $\gamma-FeOOH$ , $\alpha-FeOOH$ $\gamma-Fe_2O_3$
90	$Fe_3O_4$ $\alpha-FeOOH$ $\gamma-Fe_2O_3$

reported for iron [10], to be the boarder between the domain of chemical reactions ( $R_H < 60\%$ ) and the domain of electrochemical reactions ( $R_H > 60\%$ ). In the present work, it clearly appears a drastic mass increase at  $R_H$  values above 70%, though at the lower value of 50%, the amount of water adsorbed on the surface seems sufficient to induce electrochemical reactions.

The rate of growth of the corrosion products (at  $R_H\% > 70\%$ ) is maximum in the period 2 described above. The porosity of the corrosion products formed during this period is determining for the transport of the reacting species. At  $R_H$  values below 70%, the joint action of an impervious surface layer made of magnetite and maghemite, and of an

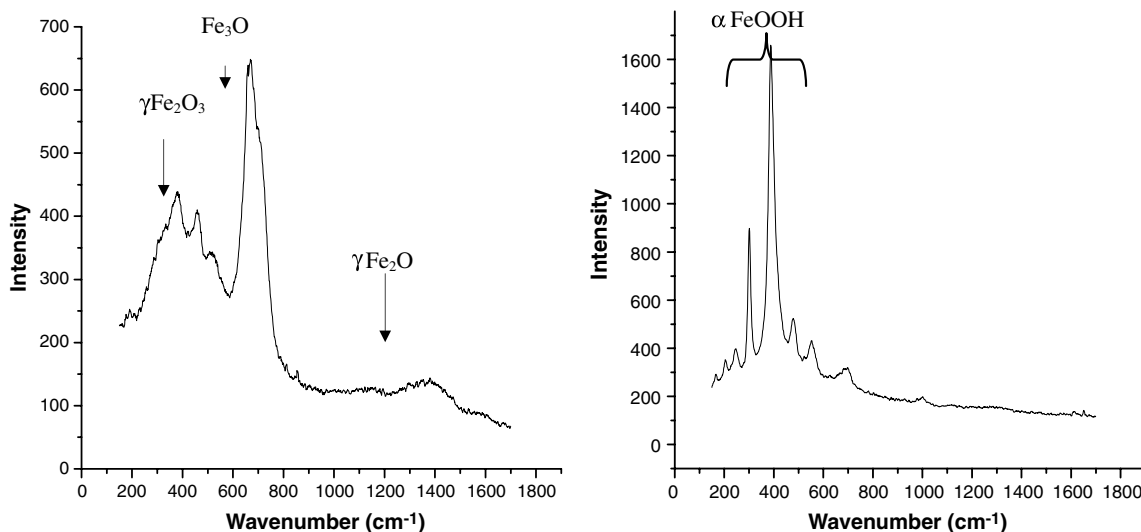


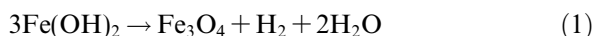
Fig. 4. Raman analysis of a quartz exposed at 343 K in the presence of 20%  $O_2$  and 90%  $R_H$  during 15 days.

insufficient water amount explains that electrochemical reactions are hindered. At higher  $R_H$  values, the corrosion layer is first expected to be very porous, allowing the formation of hydrated oxides (lepidocrocite, goethite) at the oxide/water interface. These hydrated species progressively plug up the pores [11], leading to the slow down of the rate of oxide growth clearly observed in period 3 at 70%  $R_H$ . A trend of slowing down is also observed at 80%  $R_H$ , but experiments should be performed during a longer time to verify the efficiency of the pore-blocking mechanism. Unfortunately, the QCM method used in this work does not allow the consumption of high amounts of iron, as it was shown above at 90%  $R_H$ . Measurements on bulk steel coupons are in progress for the long-term behaviour, in the most corrosive conditions.

### 3.1.2. Influence of temperature at 70% $R_H$

As already mentioned, the exact operative conditions for final disposal are yet not known. In what follows, a relative humidity of 70% was chosen for temperature effects investigations: 70%  $R_H$  is high enough to induce electrochemical corrosion, and low enough to avoid local dissolution of the iron deposit used during this study.

Experiments were performed at 323, 343 and 363 K for 70%  $R_H$ . The mass first increased in the 298–323 K temperature range, then decreased from 323 to 363 K. According to Lee and Staehle [11], the amount of adsorbed water at the surface of a iron mainly depends on the value of the relative humidity in the 280–358 K temperature range. Thus the amount of adsorbed water at 70%  $R_H$  is assumed to be constant whatever the temperature of the chamber. An increase of the temperature generally leads to an activation of the chemical and electrochemical reactions. The increase in mass observed between 298 and 323 K is thus easy to understand. More surprising is the decrease in the rate of corrosion, as the temperature increases from 323 to 363 K. A decrease in the rate of corrosion when the temperature increases has been observed in fully anoxic conditions at temperatures greater than 323–333 K, and has been attributed to transformation of ferrous hydroxide into magnetite [12], according to



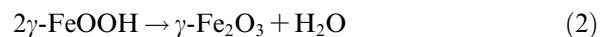
To our knowledge, a decrease of the rate of corrosion, in the presence of oxygen and when the temperature increases has never been discussed.

Mabuchi et al. [6] have estimated the rate of dissolution and the film thickness formed on iron after 4 days of immersion in water at high temperature. They found that when temperature increases from 333 to 523 K, the rate of corrosion passes through a minimum depending on oxygen content. But no interpretation has been given.

In the present work, optical observations showed that the corrosion layers obtained at temperatures between 298 and 323 K were loose and porous, whereas corrosion layers formed at 363 K appear to be more adherent than those formed at 323 K. Moreover, Raman spectrometry analyses (Table 3) showed that magnetite, maghemite and hydroxides are the main components of the rust at 323 and 343 K, but that only magnetite and maghemite were detected at 363 K.

Two possible explanations can be given for the decrease of the corrosion rate with increasing temperature. The first one is that at a given  $R_H$ % value, the thickness of the water layer deposited on the iron or on the iron oxides decreases with increasing temperature. This assumption would be in contradiction with Refs. [11,13], but would be in agreement with the Raman spectrometric analyses showing that no hydroxide but only magnetite or maghemite is formed at 363 K (as was observed at 50%  $R_H$ ).

An other explanation, in agreement with the Raman spectrometric analyses, would be that an increase in temperature leads to the transformation of lepidocrocite into maghemite in the solid phase according to



This assumption is also in agreement with the potential-pH diagrams [14] established in the temperature range from 298 to 423 K, showing that oxides ( $\text{Fe}_3\text{O}_4$  and  $\text{Fe}_2\text{O}_3$ ) are more stable than hydroxides at temperature above 343 K.

Table 3  
Oxides and hydroxides phases detected by Raman spectroscopy for experiments performed at 323 and 363 K and for 70%  $R_H$ –20%  $\text{O}_2$

Temperature (K)	Phases detected by Raman spectroscopy
323	$\text{Fe}_3\text{O}_4$ $\gamma\text{-FeOOH}$ $\gamma\text{-Fe}_2\text{O}_3$
363	$\text{Fe}_3\text{O}_4$ $\gamma\text{-Fe}_2\text{O}_3$

### 3.2. Influence of the oxygen content at 343 K and 90% $R_H$

During the disposal of the radioactive waste containers in closed galleries, the initial oxygen concentration is expected to decrease more or less rapidly. Experiments were thus performed with different oxygen contents at a temperature of 343 K and for 90%  $R_H$ . The mass variation of the quartz exposed in such conditions is reported in Fig. 5, for oxygen contents of 1%, 5% and 20%. During period 2, the rate of growth which is about  $35 \mu\text{m yr}^{-1}$  in the presence of 20%  $\text{O}_2$ , decreases to  $10 \mu\text{m yr}^{-1}$  when the oxygen content is 5%. A rough optical estimation of the surface coverage showed that at 5% oxygen content, the surface coverage  $\theta$  is about 45%, which is a higher value than at 20% oxygen content for which  $\theta = 20\%$  (see Table 1), indicating that the corrosion products are more spread out at the surface of the quartz in the presence of lower oxygen content. It may be postulated that oxygen plays a determining role in the formation of the initially corrosion resistant zones at the metal surface. At 1% oxygen content, period 2 is very short in time (less than one day) and the surface coverage can be estimated to be about 5%. In this case, the oxygen concentration becomes too low to induce corrosion on the initially poorly protective oxide layer.

A clear stabilization of the rate of growth (period 3) is observed at the lower oxygen content (1%). As previously the rate of mass increase can be calculated taking the slope of the curve and the corresponding decrease in thickness of the metal is about  $0.12 \mu\text{m yr}^{-1}$ . This value is slightly higher

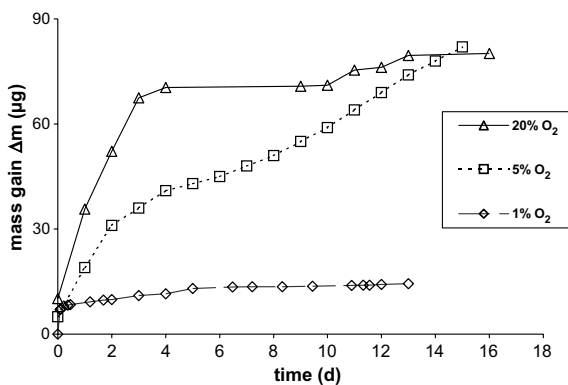


Fig. 5. Mass gain at 343 K and 90%  $R_H$  for different oxygen concentrations. Experimental results and fitted curves.

than the estimation of  $<0.1 \mu\text{m yr}^{-1}$  reported in [12] in fully anoxic conditions in bulk water. At 5% oxygen content, as was also found for 20% oxygen no stabilization was reached after 15 days of exposure, indicating that a non-protective film is formed. The exposure was not carried on, since complete dissolution of the thin iron deposit under the corrosion products could occur for a mass gain above  $70 \mu\text{g}$ .

From surface analyses using Raman Spectrometry, it appears that for the three oxygen contents, the rust layer is magnetite, maghemite and hydroxides. These results are in agreement with those obtained in bulk water in the temperature ranging from 333 to 523 K by Mabuchi et al. [6], who identified iron (III) oxides and hydroxides for oxygen contents as low as 500 ppb.

## 4. Conclusion

Atmospheric corrosion phenomena were followed using a QCM disposed in a climatic chamber. The formation of the corrosion layer was followed with time as a function of  $R_H$ , temperature and oxygen content. The influence of the relative humidity was studied at 343 K and for an oxygen content of 20 vol.%, and an exponential rate of oxide growth with  $R_H$  could be evidenced during the first days of exposure. A decrease in the rate of corrosion occurred and a phase of stabilization was obtained with a rate of iron consumption of 0.04 and  $0.23 \mu\text{m yr}^{-1}$ , respectively at 50% and 70%  $R_H$ . At higher  $R_H$  values (80% and 90%) serious corrosion was observed in form of rust zones which grew in thickness, leading to local dissolution of the iron deposit.

At a given  $R_H$  value (70%), the increase of the temperature from 298 to 363 K lead first to an increase of the mass of corrosion products from 298 to 323 K and then to a decrease when the temperature increased from 323 to 363 K. The reason for this behaviour is yet not quite clear, but can be correlated with the modification of the composition of the corrosion layer.

Experiments performed with different oxygen contents (20%, 5% and 1%), at 343 K and for 90%  $R_H$ , showed that a stabilization of the rate of growth after 15 days of exposure was only observed at the lower oxygen content (1%), whereas a non-protective film was formed at oxygen contents higher than 5%, leading to local dissolution of the iron deposit.

## References

- [1] G. Santarini, in: Proceedings of the Eurocorr 2004, paper 04-KN-510, Nice, France, 2004.
- [2] Ohtsuka, K. Kubo, N. Sato, Corrosion 42 (1986) 476.
- [3] C.S. Kumai, T.M. Devine, Corrosion 61 (2005) 201.
- [4] T. Ishikawa, M. Minamigawa, K. Kandori, T. Nakayama, T. Tsubota, J. Electrochem. Soc. 151 (2004) B512.
- [5] J.E. Maslar, W.S. Hurst, W.J. Bowers, J.H. Hendricks, M.I. Aquino, J. Electrochem. Soc. 147 (2000) 2532.
- [6] K. Mabuchi, Y. Horii, H. Takahashi, M. Nagayama, Corrosion 47 (1991) 500.
- [7] T. Aastrup, M. Wadsak, M. Schreiner, C. Leygraf, Corr. Sci. 42 (2000) 957.
- [8] J.F. Dante, R.G. Kelly, J. Electrochem. Soc. 140 (1993) 1890.
- [9] C. Leygraf, T.E. Graedel, Atmospheric Corrosion, John Wiley, New York, 2000, p. 10.
- [10] M. Tullmin, P.R. Roberge, in: R. Winston Revie (Ed.), Uhlig's Corrosion Handbook, 2nd Ed., John Wiley, New York, 2000, p. 309.
- [11] S. Lee, R.W. Staehle, Corrosion 53 (1997) 33.
- [12] N.R. Smart, D.J. Blackwood, L. Werme, Technical Report of Swedish Nuclear Fuel and Waste Management Co. TR-01-22 Stockholm, 2001, p. 8.
- [13] S.P. Sharma, J. Vac. Sci. Technol. 16 (1979) 1557.
- [14] J. Chivot, Thermodynamique des produits de corrosion, Sciences et Techniques Series, ANDRA, 2004, p. 4.